Supporting information for: Absorbate-induced piezochromism in a porous molecular crystal

Christopher H. Hendon,[†] Kate E. Wittering,[‡] Teng-Hao Chen,[¶] Watchareeya Kaveevivitchai,[¶] Ilya Popov,[¶] Keith T. Butler,[†] Chick C. Wilson,[†] Dyanne L. Cruickshank,[*,§] Ognjen Š. Miljanić,[*,¶] and Aron Walsh[*,†]

Department of Chemistry, University of Bath, Claverton Down, Bath, BA2 7AY, UK, CMAC, EPSRC Centre for Continuous Manufacturing and Crystallisation, Department of Chemistry, University of Bath, Bath, BA2 7AY, Department of Chemistry, University of Houston, 112 Fleming Building, Houston, Texas 77204-5003, USA, and Centre for Supramolecular Chemistry Research, Department of Chemistry, University of Cape Town, Rondebosch, 7701, South Africa

E-mail: dyanne.cruickshank@uct.ac.za; miljanic@uh.edu; a.walsh@bath.ac.uk

[*]To whom correspondence should be addressed

[†]Department of Chemistry, University of Bath, Claverton Down, Bath, BA2 7AY, UK

[‡]CMAC, EPSRC Centre for Continuous Manufacturing and Crystallisation, Department of Chemistry, University of Bath, Bath, BA2 7AY

[¶]Department of Chemistry, University of Houston, 112 Fleming Building, Houston, Texas 77204-5003, USA

[§]Centre for Supramolecular Chemistry Research, Department of Chemistry, University of Cape Town, Rondebosch, 7701, South Africa

Computational Methods

Periodic Calculations

To calculate the reference electrostatic potential (vacuum level) we take a spherical average of the Hartree potential in a sphere of radius 2 Å with an origin at the centre of the pore.[1] The electrostatic potential is spherically sampled, illustrated in Figure S1a. Furthermore, the electrostatic potential contour map is shown in Figure S1b. The analysis code for this calculation, which can also calculate planar and macroscopic averages of electrostatic potentials and charge densities, is freely available.[2]

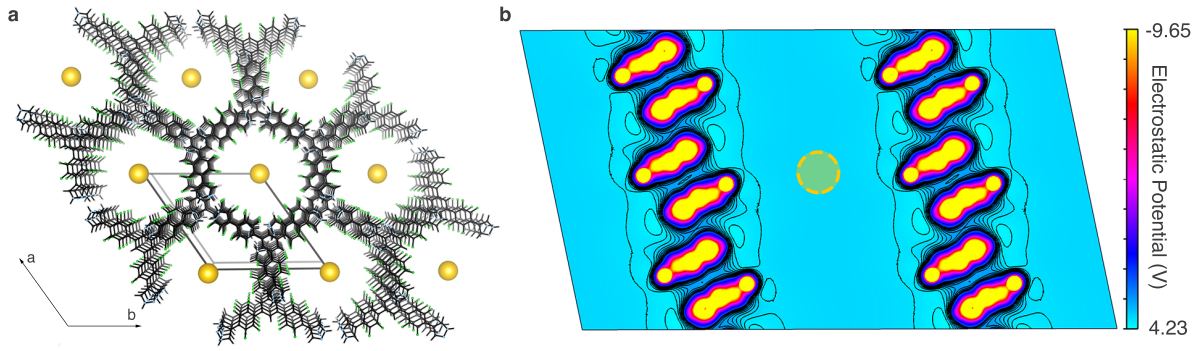

Figure S1: The porous molecular crystal, **1** (**a**), depicted with the electrostatic potential sampling region in the sphere. The electrostatic potential (V) may be mapped through any lattice plane; the [010] of the $C2/c$ setting is shown with the sampling region represented by the circle in the center of the pore, **b**.

The electronic structure was calculated for all systems within Kohn-Sham density functional theory (DFT). The Vienna *ab initio* simulation package (*VASP*),[3] a plane-wave basis set code (with projected augmented wave (PAW) scalar-relativistic pseudopotentials), was employed for crystal and electronic structure optimisation with Γ-point sampling of the first Brillouin zone. A 500 eV plane-wave cut-off was employed. All unit cell vectors and internal positions were relaxed to their equilibrium values, starting with the experimentally determined structure.[4] The PBEsol[5] functional produces optimised structures with lattice parameters within 1% of experiment.

All electronic properties, including electron density, electrostatic potential and band gap,

were computed using a hybrid exchange-correlation functional (HSE06)[6,7] with 25% of the short-range semi-local exchange replaced by the non-local Hartree-Fock exchange.

From the original report, **1** crystallises in the *C2/c* space group, however we collected a second set of data and found a preffered space group setting of *I2/a*. The refinement parameters were superior to the previously published structure. Electronic structure calculations were computed on an associated primitive cell, which is approximately half the size. The energy-volume response functions were calculated by applying hydrostatic pressure to the equilibrated primitive cell, sampling a range of volumes (±1 %) in steps of 0.1 %. The geometric deformation of both the ionic positions and cell shape were computed with the PBEsol functional for the varying pressures. The geometric unit cell shape and internal ionic positions were relaxed for each pressure, and the electronic structure was subsequently calculated using the HSE06 functional.

Table S1: Changes in bond lengths and lattice parameters with change in cell volume.

Identifier	Volume (Å^3)	**a** (Å)	**b** (Å)	**c** (Å)	N$\cdots$N$^{[a]}$ (Å)	C$\cdots$C$^{[b]}$ (Å)	$\pi\cdots\pi^{[c]}$ (Å)
71 MPa	6404	19.609	19.611	21.759	2.721	1.401	3.614
36 MPa	6602	19.637	19.632	22.088	2.735	1.402	3.683
0 MPa	6804	19.675	19.668	22.494	2.756	1.402	3.734
-37 MPa	7010	19.697	19.689	22.991	2.773	1.403	3.815
-74 MPa	7220	19.699	19.695	23.527	2.782	1.403	3.905
1*	6780	19.830	19.830	22.045	2.784	1.390	3.697

$^{[a]}$ = Heavy atom hydrogen-bond length $^{[b]}$ = Average aromatic ring length $^{[c]}$ = π-stacking length
* = Experimental values for the primitive cell

Single Molecule Calculations

Calculations of the highest occupied and lowest unoccupied molecular orbitals were performed using the FHI-aims package.[8] Within this all-electron approach the electronic wavefunctions are constructed using numeric atom-centred basis functions. A converged 'tight' basis set was employed, which includes d, f and g functions on atoms heavier than, or equal to oxygen, and scalar relativistic effects were included.

Local structure optimisation were performed using the forces from DFT using the PBE

exchange-correlation potential.[9] For more accurate electronic structure calculations, the HSE06 functional used in the periodic calculations was applied to the structure obtained from the PBE optimisation. Given the periodic calculations show consistent agreement with experiment using the HSE06 functional, we elected to use the same functional (which also generated reliable results in the single molecule case).

Synthesis and Characterisation

1 was synthesised using the recently published procedure outlined by Miljanić and co-workers.[4] The samples were evacuated under vacuum at 80 ^{o}C for 12 hours. Fluorescence measurements were performed by using a PTI QuantaMaster QM4 CW spectrofluorometer. The absorption and emission spectra were recorded in the solid state at room temperature.

Crystallinity of the vacuous and loaded samples were confirmed with flat-plate PXRD, collected in flat-plate mode on a Bruker D8 Advance equipped with monochromated Cu-K$_\alpha$ radiation (λ=1.54056 Å) in reflection geometry at 298 K. Capillary PXRD was used to probe temperature dependence using an Agilent SuperNova diffractometer with Cu-K$_\alpha$ radiation (λ=1.54056 Å).

Single crystal data and cell checks were performed using the following proceedure, and the single crystal collection of the evacuated **1** is described below.

X-ray crystallographic analysis of compound 1

Single crystal X-ray data was recorded on an Agilent Gemini A-Ultra diffractometer using Mo-K$_\alpha$ radiation (λ = 0.71073 Å). A colourless hexagonal crystal was mounted on a loop and cooled to 150(2) K by an Agilent Cryojet system. Indexing and unit cell refinement indicated an I-centered, monoclinic lattice. The space group was found to be *I2/a*. The structure was solved with SHELXS-97 which revealed all non-hydrogen atoms. The atoms were placed and refined isotropically initially, and subsequently refined anisotropically. All the hydrogen atoms were placed in idealised positions based on a riding model. They were

Table S2: Crystal data and structure refinement for the evacuated **1**.

Formula weight	720.49		
Temperature (K)	150(2)		
Wavelength (Å)	0.71073		
Crystal system	monoclinic		
Space group	$I2/a$		
Unit cell dimensions (Å, °)	a = 7.3673(7)	α = 90.00	
	b = 34.542(2)	β = 91.558(10)	
	c = 18.225(2)	γ = 90.00	
Volume (Å^3)	4636.1(7)		
Z	4		
Calculated density (g·cm^3)	1.032		
Absorption coefficient (mm^{-1})	0.097		
F_{000}	1440		
Crystal size (mm)	0.10 × 0.09 × 0.05		
Θ range for data collection (°)	2.83 to 25.35		
Miller index ranges	-8 ≤ h ≤ 8	-35 ≤ k ≤ 41	-21 ≤ l ≤ 20
Reflections collected	13449		
Independent reflections	4239 [R_{int} = 0.1315]		
Completeness to Θ_{max} (%)	99.8		
Max. and min. transmission	1 and 0.9624		
Refinement method	Full-matrix least-squares on F^2		
Data, restraints, parameters	4239	0	233
Goodness-of-fit on F^2	0.955		
Final R indices [I > 2σ(I)]	R_1 = 0.0722	wR_2 = 0.1429	
R indices (all data)	R_1 = 0.1817	wR_2 = 0.1864	
Largest diff. peak and hole (e·Å^3)	0.256	-0.218	

refined isotropically with temperature factors related to those of the parent atoms to which they were attached. Both nitrogen atoms of the pyrazole rings were refined with hydrogen atoms containing site occupancy factors of a half each. This was to account for the clockwise and ant-clockwise arrangement of the hydrogen bonded trimer that forms when the molecules pack along the bc-plane. There was evidence for both hydrogen atom positions being present in the difference Fourier map.

Response to checkCIF alerts. The crystallographic information file (CIF) associated with the single crystal X-ray structure of compound 1 was subjected to IUCr's checkCIF routine which identified one A alert and no B alerts.

PLAT602_ALERT_2_A VERY LARGE Solvent Accessible VOID(S) in Structure ! Info

The evacuated **1** is composed of light elements only and arranges in such a way that there are large pores that could be filled with solvents. The sample used for single crystal X-ray diffraction was placed under a vacuum for four hours before being analysed. The pores were determined to be vacuous. The final crystal structure only contains two low electron density peaks (*ca.* 0.2 e·Å^{-3}) in the difference Fourier map which are located towards the outer edge of the vacant pores. The SQUEEZE routine was not used.

References

(1) Butler, K. T.; Hendon, C. H.; Walsh, A. *J. Am. Chem. Soc.* **2014**, *136*, 2703–2706.

(2) https://github.com/WMD-Bath/MacroDensity (Accessed 24/04/2014).

(3) Kresse, G.; Furthmüller, J. *Phys. Rev. B* **1996**, *54*, 11169.

(4) Chen, T.-H.; Popov, I.; Kaveevivitchai, W.; Chuang, Y.-C.; Chen, Y.-S.; Daugulis, O.; Jacobson, A. J.; Miljanić, O. Š. *Nature Commun.* **2014**, *5*, 5131.

(5) Perdew, J. P.; Ruzsinszky, A.; Csonka, G. I.; Vydrov, O. A.; Scuseria, G. E.; Constantin, L. A.; Zhou, X.; Burke, K. *Phys. Rev. Lett.* **2008**, *100*, 136406.

(6) Heyd, J.; Scuseria, G. E.; Ernzerhof, M. *J. Chem. Phys.* **2003**, *118*, 8207.

(7) Krukau, A. V.; Vydrov, O. A.; Izmaylov, A. F.; Scuseria, G. E. *J. Chem. Phys.* **2006**, *125*, 224106.

(8) Blum, V.; Gehrke, R.; Hanke, F.; Havu, P.; Havu, V.; Ren, X.; Reuter, K.; Scheffler, M. *Comput. Phys. Commun.* **2009**, *180*, 2175.

(9) Perdew, J. P.; Burke, K.; Ernzerhof, M. *Phys. Rev. Lett.* **1996**, *77*, 3865.